

# Effect of collision dephasing on atomic evolutions in a high- $Q$ cavity

T.W. Chen and P.T. Leung

*Department of Physics,*

*The Chinese University of Hong Kong,*

*Shatin, Hong Kong SAR, China*

(Dated: November 10, 2018)

## Abstract

The decoherence mechanism of a single atom inside a high- $Q$  cavity is studied, and the results are compared with experimental observations performed by M. Brune *et al.* [Phys. Rev. Lett. **76**, 1800 (1996)]. Collision dephasing and cavity leakage are considered as the major sources giving rise to decoherence effect. In particular, we show that the experimental data can be fitted very well by assuming suitable values of collision Stark shifts and dark count rate in the detector.

PACS numbers: 42.50.Pq, 42.50.Xa, 42.50.Ct

A two-level atom interacting with a single cavity mode, the Jaynes-Cummings model (JCM) [1], is possibly the most well studied system in quantum optics and has the potentiality to constitute the basic building block of quantum computers [2]. Among all the intriguing phenomena related to the JCM, the oscillation in the atomic inversion probability — the Rabi oscillation — plays a prominent part in quantum optics. From a fundamental point of view, the existence of discrete Rabi frequencies provides a direct evidence of electromagnetic field quantization [1]. In particular, when there is a dispersion in the photon number, the beating of different Rabi frequencies gives rise to collapses and revivals in the inversion probability of the atom [3]. For example, if an atom initially prepared in its excited state  $|e\rangle$  evolves under the influence of a cavity field, characterized by a photon number distribution  $p_n$  and a Rabi frequency  $\Omega$ , the probability of finding the atom in the ground state  $|g\rangle$  at a later time  $t$  is given by

$$P_{eg}(t) = \frac{1}{2} \sum_{n=0}^{\infty} p_n \left[ 1 - \cos \left( 2\Omega t \sqrt{n+1} \right) \right], \quad (1)$$

which clearly demonstrates the mentioned phenomenon.

The first observation of quantum Rabi oscillation was made by Rempe *et al.* some years ago [4]. However, their experiment failed to obtain a conclusive result due to the limitation on the observation time. More recently, M. Brune *et al.* successfully carried out an experiment to observe the Rabi oscillation [5], which for the first time provided direct and clear evidence of field quantization inside a high- $Q$  cavity. In their experiment, Rydberg atoms independently interact with a photon mode in a superconducting microwave cavity and undergo transitions between two atomic states with principal quantum numbers 51 and 50 respectively. The  $Q$ -factor of the cavity mode is  $7 \times 10^7$ , which corresponds to a photon lifetime of  $220 \mu\text{s}$ . The Rabi frequency at the center of the cavity is  $\Omega_0 = 50\pi \text{ kHz}$ , which is sufficiently fast to make Rabi oscillations observable within the cavity leakage time. The atoms are initially prepared in the excited state and, in addition to a background 0.8 K thermal field with a mean photon number  $\bar{n}_{\text{th}} \simeq 0.06$ , the cavity field is maintained in coherent states with mean photon number  $\bar{n}$  varying from zero to a few photons. The experimental data of  $P_{eg}$  obtained from Ref. [5], for  $\bar{n} = 0, 0.4, 0.85$  and  $1.77$  are reproduced here as the boxes in Figs. 1-4. Despite that the data clearly revealed the Rabi oscillations in  $P_{eg}(t)$ , the evolution does not conform to that predicted by Eq. (1) (solid lines in Fig. 1).

Instead, it was shown that a best fit to the data is given by [5]:

$$P_{eg}(t) = \frac{1}{2} \sum_{n=0}^{\infty} p_n \left[ 1 - \exp(-\Gamma t) \cos \left( 2\Omega t \sqrt{n+1} \right) \right]. \quad (2)$$

The oscillations were damped in such a way that  $P_{eg}(t)$  approached 0.5 in the long term. This behavior is not attributable to cavity leakage, which would instead lead to  $P_{eg}(t) = 1$  asymptotically. Furthermore, the photon lifetime was actually longer than the observation time and the effect of cavity damping due to leakage should only play a marginal role (see the dot-dashed lines in Fig. 1). It was conjectured that decoherence effect due to collisions with background gas might have contributed to these damped oscillations [5].

The aim of this report is to theoretically account for the experimental results by studying the effects of collision dephasing and cavity leakage. We will show in the following discussion that these two independent mechanisms are the main culprits leading to the discrepancy between the experimental data and the theoretical results given by Eq. (1).

In the rotating wave approximation, the hamiltonian of a two-level atom interacting with an ideal cavity mode is given by (in units of  $\hbar = 1$ ):

$$H_0 = \frac{\omega_a}{2} S_z + \omega_c a^\dagger a + \Omega \left( a^\dagger S_- + a S_+ \right), \quad (3)$$

where  $a^\dagger$  and  $a$  are respectively the creation and annihilation operators of the cavity field,  $S_z$  and  $S_\pm$  are the pseudo-spin operators of the atomic levels, and  $\omega_a$  and  $\omega_c$  are the atomic transition and cavity mode frequencies respectively. Hereafter, we will assume exact resonance condition such that  $\omega_a = \omega_c$ . It is worthwhile to note that the vacuum Rabi frequency  $\Omega$  in the hamiltonian can be smaller than the maximum Rabi frequency  $\Omega_0$  because maximum coupling is attainable only if the two-level atoms are exactly located at the cavity center [5]. Instead,  $\Omega$  will be considered as a free parameter to fit the leading few Rabi oscillations.

To include the effects of collision dephasing and cavity leakage on the system, we consider the master equation for the density matrix  $\rho$  [6, 7]:

$$\frac{\partial \rho}{\partial t} = -i [H_0, \rho] + L_c \rho + L_f \rho, \quad (4)$$

where

$$L_f \rho = \frac{\kappa}{2} (2a\rho a^\dagger - a^\dagger a \rho - \rho a^\dagger a), \quad (5)$$

with  $\kappa$  being the cavity leakage rate ( $\kappa = 4.55$  kHz in the experiment), and

$$L_c \rho = 2\gamma (2S_z \rho S_z - S_z^2 \rho - \rho S_z^2). \quad (6)$$

The operator  $L_f$  results from finite leakage at the boundaries of the cavity, whereas  $L_c$  describes the effect of collision dephasing characterized with an energy shift  $2\gamma$  [6, 7]. In general, there is an additional term due to spontaneous decay:

$$L_s\rho = -\frac{\Gamma_e - \Gamma_g}{2}\{S_z, \rho\} - \frac{\Gamma_e + \Gamma_g}{2}\rho, \quad (7)$$

with  $\Gamma_e$  and  $\Gamma_g$  being the spontaneous decay rates of the upper and lower energy levels respectively. However, in the experiment the lifetimes of the two levels are about 30 ms [5], which are relatively long compared with the atom-cavity interaction time, and this term is ignored hereafter. Besides, we also assume that the thermal field outside the cavity is negligible. In terms of the density matrix,  $P_{eg}(t)$  is given by

$$P_{eg}(t) = \sum_n \langle n, g | \rho | n, g \rangle. \quad (8)$$

In the current situation, the leakage of the cavity is small. It is legitimate to take  $L_f\rho$  as the small term and Eq. (4) can then be solved by method of perturbation. First, the density matrix is written as

$$\rho = \rho^{(0)} + \rho^{(1)}, \quad (9)$$

where  $\rho^{(1)}$  is a small correction to the zeroth order density matrix  $\rho^{(0)}$ . It is then readily shown that

$$\frac{\partial \rho^{(0)}}{\partial t} = -i [H_0, \rho^{(0)}] + L_c \rho^{(0)}, \quad (10)$$

and

$$\frac{\partial \rho^{(1)}}{\partial t} = -i [H_0, \rho^{(1)}] + L_c \rho^{(1)} + L_f \rho^{(0)}. \quad (11)$$

Secondly, we solve Eq. (10) for the initial conditions:

$$\begin{aligned} \langle n, e | \rho^{(0)} | n, e \rangle &= p_n, \\ \langle n, g | \rho^{(0)} | n, g \rangle &= \langle n, e | \rho^{(0)} | n+1, g \rangle = \langle n+1, g | \rho^{(0)} | n, e \rangle = 0. \end{aligned}$$

When the field is prepared in a coherent state, the photon distribution is Poissonian with  $p_n$  given by:

$$p_n = e^{-\bar{n}} \frac{\bar{n}^n}{n!}. \quad (12)$$

The explicit solution to Eq. (10) is:

$$\langle 0, g | \rho^{(0)} | 0, g \rangle = 0, \quad (13)$$

$$\langle n, g | \rho^{(0)} | n, g \rangle = \frac{1}{2} p_{n-1} \left[ 1 - \exp(-\gamma t) \frac{\cos(\lambda_{n-1} t - \phi_{n-1})}{\cos \phi_{n-1}} \right], \quad (14)$$

$$\langle n, e | \rho^{(0)} | n, e \rangle = \frac{1}{2} p_n \left[ 1 + \exp(-\gamma t) \frac{\cos(\lambda_n t - \phi_n)}{\cos \phi_n} \right], \quad (15)$$

$$\langle n, e | \rho^{(0)} | n+1, g \rangle = \frac{i}{2} p_n \exp(-\gamma t) \frac{\sin \lambda_n t}{\cos \phi_n}, \quad (16)$$

where

$$\lambda_n = \sqrt{4(n+1)\Omega^2 - \gamma^2} \quad (17)$$

and

$$\tan \phi_n = \frac{\gamma}{\lambda_n}. \quad (18)$$

Eq. (8) can hence be expressed explicitly as

$$P_{eg}(t) = \frac{1}{2} \sum_{n=0}^{\infty} p_n \left[ 1 - \exp(-\gamma t) \frac{\cos(\lambda_n t - \phi_n)}{\cos \phi_n} \right]. \quad (19)$$

From the results, we see that the mechanism of collision dephasing gives rise to remarkable effects. The Rabi oscillations are damped with modified frequencies given by Eq. (17); and there is also a phase shift as given by Eq. (18). The solid-lines in Fig. 2 show the zeroth order perturbation results for  $\Omega_0 = 150.2$  kHz and  $\gamma = 19.3$  kHz, which is observed to provide best fits to the four sets of experimental data. The results obtained by numerically solving the exact master equation (i.e. Eq. (4)) are also shown there as dot-dashed lines. Interestingly enough, there is a fairly good apparent agreement between the zeroth order results and the experimental data. We consider this as a coincidence due to two counter-balancing effects, namely the effects of cavity leakage and dark counts in the detector used in the experiment [5], which have been neglected in the forgoing discussion. We will return to this point later.

To obtain a better agreement between the perturbative and the numerical results, the first order calculation is carried out, yielding the results:

$$\langle 0, g | \rho^{(1)} | 0, g \rangle = -\frac{\kappa}{4\Omega} p_0 \left[ 2 \sin \phi_0 - 2\Omega t + \exp(-\gamma t) \frac{\sin(\lambda_0 t - 2\phi_0)}{\cos \phi_0} \right], \quad (20)$$

$$\begin{aligned} & \langle n, g | \rho^{(1)} | n, g \rangle \\ &= \kappa \frac{\sin 2\phi_n}{4n\lambda_n} p_{n-1} + \frac{1}{4} [(2n+1)p_n - (2n-1)p_{n-1}] \kappa t \\ & \quad - \kappa \exp(-\gamma t) \left\{ (2n^2 + n + 1) p_n \frac{\sin 2\phi_{n-1}}{4\lambda_{n-1}} \cos \lambda_{n-1} t \right. \end{aligned}$$

$$\begin{aligned}
& - \frac{(2n-1)(1-\sqrt{n})p_{n-1} + [4n^2 + 3n + 1 - 2(4n^2 + 2n + 1)\sin^2\phi_{n-1}]p_n}{4\lambda_{n-1}} \sin\lambda_{n-1}t \\
& + \frac{n(n+1)p_n}{2\lambda_n} \sin\lambda_n t + \frac{(2n^2 + 3n + 2)p_n}{4\lambda_n} \sin(\lambda_n t - 2\phi_n) \\
& - \frac{(2n-1)\sqrt{n}p_{n-1}}{2\lambda_{n-1}} \Omega t \cos(\lambda_{n-1}t - \phi_{n-1}) \Big\}, \tag{21}
\end{aligned}$$

$$\begin{aligned}
& \langle n, e | \rho^{(1)} | n, e \rangle \\
& = \kappa \left( \frac{\sin 2\phi_n}{2\lambda_n} p_n - \frac{(2n+3)\sin 2\phi_{n+1}}{4(n+1)\lambda_{n+1}} p_{n+1} \right) + \frac{1}{4} [(2n+3)p_{n+1} - (2n+1)p_n] \kappa t \\
& + \kappa \exp(-\gamma t) \left\{ \frac{(2n^2 + 5n + 4)p_{n+1} - 2p_n}{4\lambda_n} \sin 2\phi_n \cos \lambda_n t \right. \\
& + \frac{[(2n+1)(\sqrt{n+1}-1) + 2\cos 2\phi_n] p_n - [n+1 + (4n^2 + 10n + 7)\cos 2\phi_n] p_{n+1}}{4\lambda_n} \sin \lambda_n t \\
& + \frac{(n+1)(n+2)p_{n+1}}{2\lambda_{n+1}} \sin \lambda_{n+1} t + \frac{(2n^2 + 7n + 5)p_{n+1}}{4\lambda_{n+1}} \sin(\lambda_{n+1} t - 2\phi_{n+1}) \\
& \left. - \frac{(2n+1)\sqrt{n+1}p_n}{2\lambda_n} \Omega t \cos(\lambda_n t - \phi_n) \right\}, \tag{22}
\end{aligned}$$

$$\begin{aligned}
& \langle n, e | \rho^{(1)} | n+1, g \rangle \\
& = \frac{\kappa}{8\sqrt{n+1}\Omega} (p_n - p_{n+1}) - \frac{\kappa}{8\sqrt{n+1}\Omega} \exp(-\gamma t) \left\{ [p_n - (3n^2 + 8n + 6)p_{n+1}] \cos \lambda_n t \right. \\
& + [p_n + (n^2 + 4n + 2)p_{n+1}] \tan \phi_n \sin \lambda_n t + 2(n+1)(3n+5)p_{n+1} \cos \lambda_{n+1} t \\
& \left. + 2(n+1)^2 p_{n+1} \tan \phi_{n+1} \sin \lambda_{n+1} t + 4(n+1)(2n+1)p_n \frac{\Omega^2}{\lambda_n} t \sin \lambda_n t \right\}. \tag{23}
\end{aligned}$$

The first order results with the same parameters are shown in Fig. 3. In the time regime under consideration, the first order results give excellent approximation to the exact numerical solution that includes the leakage effect. However, as shown in Fig. 3, the introduction of leakage obviously also worsens the agreement between our theoretical results and the experimental data. As suggested in Ref. [5], we propose that the effect of cavity damping might have been counter-balanced by dark counts in the atomic detector, which become increasingly important at long times because of low atomic fluxes. If it is assumed that within the time range of the experiment, the detection rate approximately goes exponentially with  $t$ , an extra factor  $e^{-\alpha t}$  should be introduced. In other words,

$$[P_{eg}(t)]_{\text{experiment}} = e^{-\alpha t} [P_{eg}(t)]_{\text{theory}}. \tag{24}$$

In the time regime under consideration, this is roughly the same as assuming a linear time dependence of the dark count rate. In order to counter-balance the effect of cavity damping, we find that  $\alpha$  should assume a value around 1.59 kHz. In other words, the proportion of dark counts should increase from 0 at  $t = 0$  to around 13% at  $t = 90 \mu\text{s}$ . In Fig. 4, the overlying solid lines and dot-dashed lines respectively show the first-order perturbation and numerical results with the effect of dark counts taken into account. It clearly shows an excellent agreement with experimental data.

Moreover, the results of the first order perturbation allow us to write Eq. (8) in the form

$$P_{eg}(t) = \sum_{n=0}^{\infty} p_n f_n(t), \quad (25)$$

where the functions  $f_n(t)$  are obtained by grouping terms in Eqs. (13)-(16) and (20)-(23). Instead of evaluating  $P_{eg}(t)$  from the given photon distribution function  $p_n$  [5], we can in fact search for initial states that best fit the data. With the set of functions  $f_n(t)$ , we perform a least-square best fit to obtain the optimal photon distribution  $\tilde{p}(n)$ . The results of this inversion process are shown by circles in Fig. 5, in which the solid lines represent the theoretical results for the initial states given in Ref. [5], namely  $\bar{n} = 0, 0.4 \pm 0.02, 0.85 \pm 0.04$  and  $1.77 \pm 0.15$ . It is observed that the results we obtained show a fairly good agreement with the theoretical values. Furthermore, we perform independent best-fits on  $p(n)$  to find the coherent states that give the best agreement. We found that the distributions are respectively best fit by coherent states with  $\bar{n} = 0.098, 0.46, 1.19$  and  $1.95$ , signifying the agreement of the experimental and theoretical results.

In conclusion, we have theoretically analyzed the evolution of a single atom inside a high- $Q$  cavity in the presence of collision dephasing and leakage mechanisms, and the results are compared with experimental observations performed by Brune *et al.* [5]. Collision dephasing, leakage and dark counts are shown to be the major factors affecting the experimental results. Interestingly enough, cavity leakage and dark counts tend to produce opposite effects on the inversion probability. By assuming suitable values of collision Stark shift and dark count rate, we have explicitly demonstrated that the experimental data agree nicely with the theoretical prediction.

## Acknowledgments

We thank G. Q. Ge and C. K. Law respectively for drawing our attention to Brune *et al.*'s experiment and discussions. Our work is supported in part by the Hong Kong Research Grants Council (grant No: CUHK4282/00P) and a direct grant (Project ID: 2060150) from the Chinese University of Hong Kong.

- 
- [1] E.T. Jaynes and F.W. Cummings, Proc. IEEE **51**, 89 (1963).
  - [2] See, for example, *The Physics of Quantum Information*, Eds. D. Bouwmeester, A. Ekert, and A. Zeilinger (Springer, Berlin, 2000).
  - [3] J.H. Eberly, N.B. Narozhny, and J.J. Sanchez-Mondragon, Phys. Rev. Lett. **44**, 1323 (1980).
  - [4] G. Rempe, H. Walther, and N. Klein, Phys. Rev. Lett. **58**, 353 (1987).
  - [5] M. Brune, F. Schmidt-Kaler, A. Maali, J. Dreyer, E. Hagley, J.M. Raimond, and S. Haroche, Phys. Rev. Lett. **76**, 1800 (1996); S. Haroche, Hyperfine Interactions **114**, 87 (1998).
  - [6] R.R. Puri, and G.S. Agarwal, Phys. Rev. A **45**, 5073 (1992).
  - [7] M.O. Scully and M.S. Zubairy, *Quantum Optics* (Cambridge University Press, Cambridge, UK, 1997).

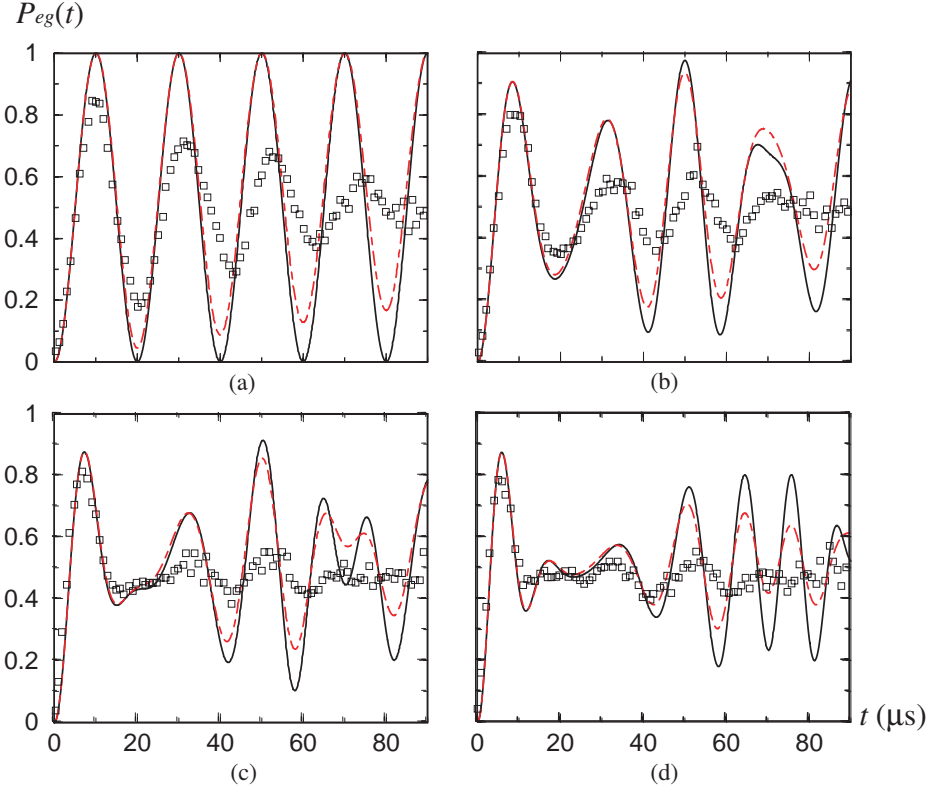


FIG. 1:  $P_{eg}(t)$  vs time for (a)  $\bar{n} = 0$ , (b)  $\bar{n} = 0.4$ , (c)  $\bar{n} = 0.85$  and (d)  $\bar{n} = 1.77$ . Boxes represent experimental data reproduced from Ref. [5]. Solid lines are the theoretical results for  $\kappa = \gamma = 0$  and  $\Omega = \Omega_0 = 50\pi$  kHz. Dot-dashed lines are the results when finite cavity damping with  $\kappa = 4.55$  kHz is taken into account.

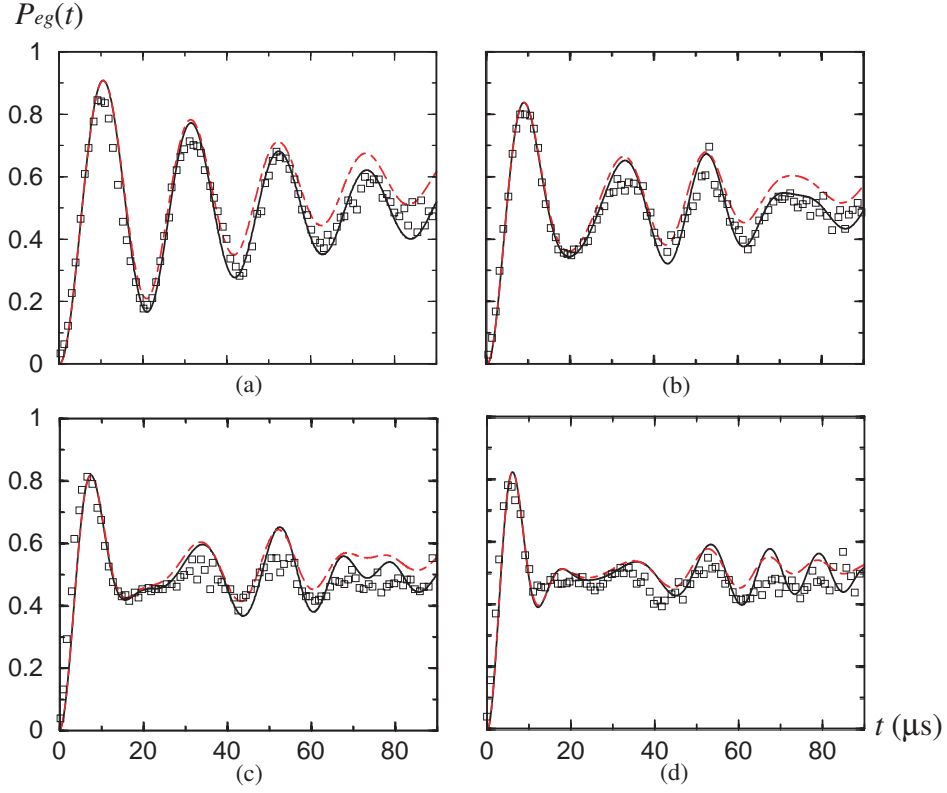


FIG. 2:  $P_{eg}(t)$  vs time for (a)  $\bar{n} = 0$ , (b)  $\bar{n} = 0.4$ , (c)  $\bar{n} = 0.85$  and (d)  $\bar{n} = 1.77$ . Boxes represent experimental data reproduced from Ref. [5]. Solid lines are the exact analytic results with collision dephasing  $\gamma = 19.3$  kHz,  $\kappa = 0$  and  $\Omega = 150.2$  kHz. Dot-dashed lines are the exact numerical results with the same set of parameters except that  $\kappa = 4.55$  kHz.

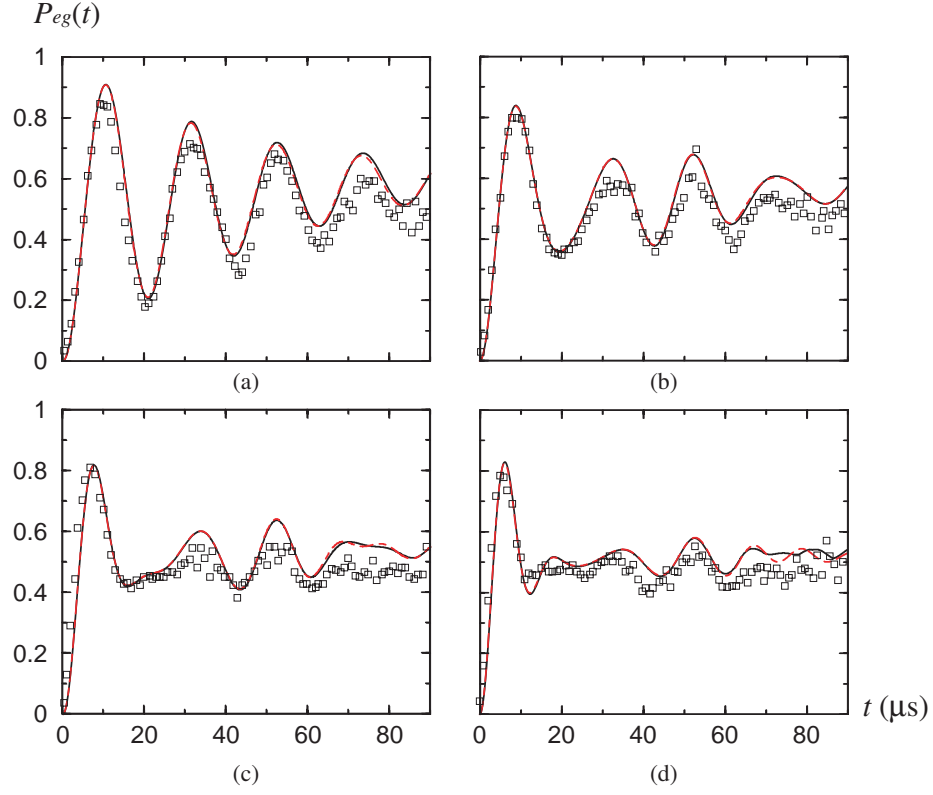


FIG. 3:  $P_{eg}(t)$  vs time for (a)  $\bar{n} = 0$ , (b)  $\bar{n} = 0.4$ , (c)  $\bar{n} = 0.85$  and (d)  $\bar{n} = 1.77$ . Boxes represent experimental data reproduced from Ref. [5]. Solid lines are the results of the first order perturbation for a case with collision dephasing  $\gamma = 19.3$  kHz,  $\kappa = 4.55$  kHz and  $\Omega = 150.2$  kHz. Dot-dashed lines are the exact numerical results.

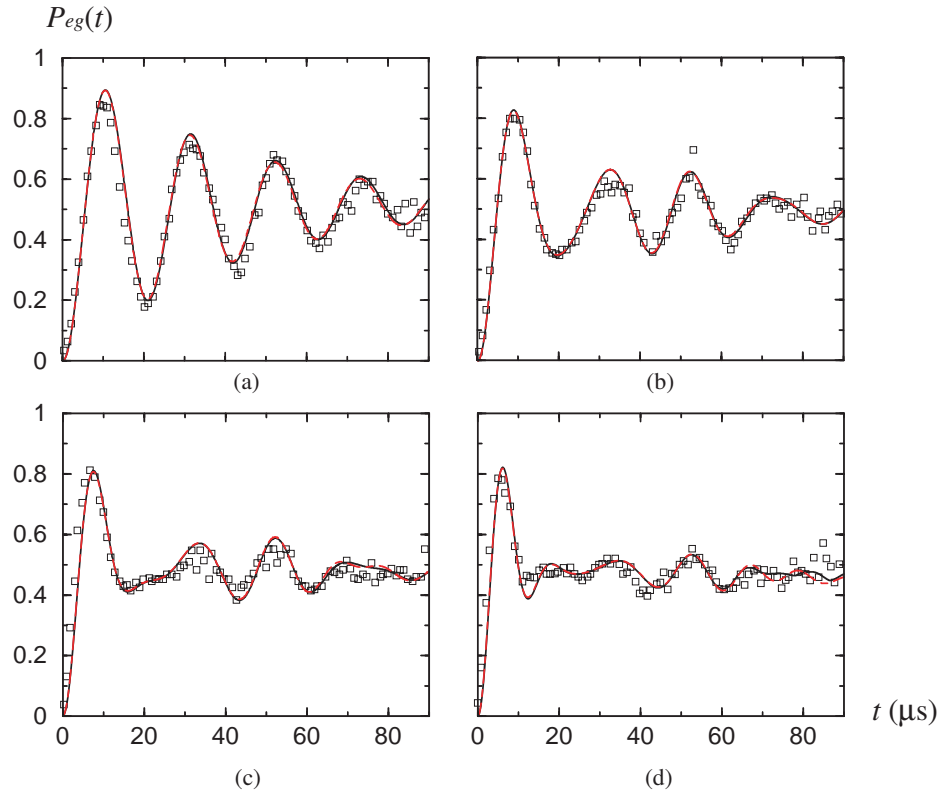


FIG. 4: Same as Fig. 3, except the introduction of dark counts with  $\alpha = 1.59$  kHz.

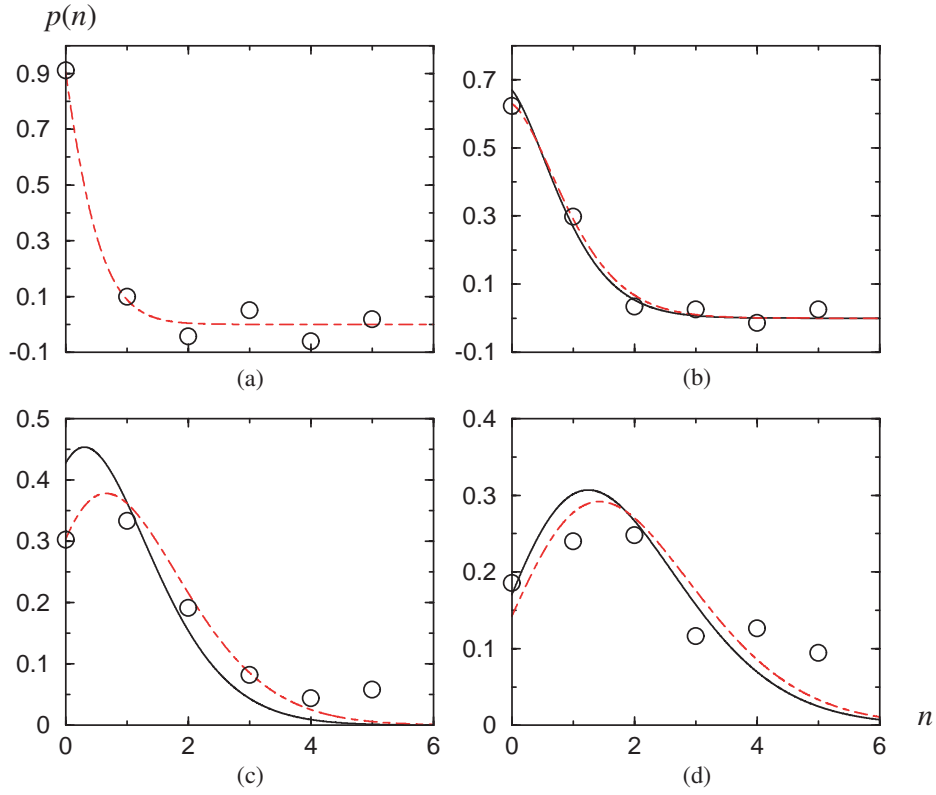


FIG. 5: Photon statistics for the four experimental situations. Circles represent the results obtained by inverting the optimal  $\tilde{p}_n$  from the experimental data. Dot-dashed lines are Poissonian distributions that best fit the circles. Solid lines are the Poissonian distributions specified in Ref. [5].